

Magneto-optic investigation of magnetic structures under micron resolution conditions

G. S. Krichik and O. M. Benidze

Moscow State University

(Submitted May 28, 1974)

Zh. Eksp. Teor. Fiz. 67, 2180-2194 (December 1974)

Iron, yttrium orthoferrite, and hematite single crystals were investigated using magneto-optic apparatus capable of micron resolution. A magneto-optic domain wall signal was obtained for iron and hematite and a study was made of the distribution of the magnetization in the volume occupied by a domain wall. The processes of magnetization and of magnetization switching in a domain wall were investigated, i.e., a study was made of the dimensions and polarity of subdomains in a domain wall in an iron whisker. The domain structure of different faces of orthoferrite and hematite single crystals was investigated and displacements of domain walls and domains as a whole were studied. A characteristic domain structure, due to the appearance of a uniaxial surface magnetism, was observed on nonbasal faces of hematite. The presence of surface magnetism was confirmed by measuring the anisotropy of the magneto-optic effect when a sample and an external magnetic field were rotated.

1. INTRODUCTION

In an earlier paper,^[1] we described magneto-optic apparatus for the investigation of the distribution of magnetization on microscopic surface regions of the order of one square micron and we demonstrated^[2] the suitability of this method in studies of real magnetic microstructure elements in ferromagnetic metals. We obtained magneto-optic signals from a domain wall in iron and nickel single crystals and from separate micron-size domains in Permalloy films with the stripe structure.

The present paper reports the results of an investigation of various elements of the magnetic structure of magnetically ordered crystals, obtained using an improved version of the micron-resolution magneto-optic apparatus described earlier. The improvements in the apparatus and method consisted of an increase in the gain and reduction in the pass band of a selective amplifier, use of a synchronous detector which made it possible to increase the sensitivity and analyze the phase of the magneto-optic signal, use of microdrives for continuous and independent movement of the entry slit of a photomultiplier in the vertical and horizontal directions in the focal plane of the microscope, use of a device with microdrives for moving a sample above the objective in two perpendicular directions and for rotating the sample about its vertical axis, increase in the light source stability, and use of a low-noise photomultiplier. Moreover, the strong magneto-optic reflection effects exhibited by ferroelectric insulators, including weak ferromagnets,^[3] made it possible to employ the proposed method in a study of the magnetic structures not only of ferromagnetic metals but also of magnetically ordered insulator crystals.

The principle of the operation of the micron-resolution magneto-optic apparatus, described in detail in^[1,2], was the determination of the change in the intensity of light which reached the image plane of the microscope from a micron-size surface area of an investigated sample. The magneto-optic effect determined experimentally was a measure of the change in the magnetization of the illuminated surface region due to periodic variation of an external magnetic field. The transition from one magneto-optic effect to another by a change in the orientation of the sample as well as the plane and angle of incidence of light and the introduction of an

analyzer made it possible, at least in principle, to determine the contributions of all the components of the magnetization. Important information was also obtained when the amplitude of the external magnetic field was varied.

The capabilities of the method can best be illustrated by giving examples of operations which can give a particular component of the magnetization in a micro-region of the surface of a magnetic crystal.

1. When an ordinary objective is used, we obtain a symmetric beam in the sense that, for each ray of light with a positive angle of incidence, there is a ray with a negative angle which destroys the equatorial and meridional Kerr effects that are odd in respect of the angle of incidence and depend linearly on the tangential (i.e., parallel to the sample surface) components of the magnetization.

a) The introduction of an analyzer makes it possible to determine the polar Kerr effect, i.e., the change in the normal component of the magnetization.

b) In the absence of an analyzer, we can record the orientational magneto-optic effect, i.e., the change in the intensity of the reflected light proportional to the change in the square of the tangential component of the magnetization which is perpendicular to the plane of incidence of light.^[4]

2. The introduction of an obliquely illuminated prism fixes the plane and angle of incidence of light and this makes it possible to measure the magneto-optic effects which are related linearly to the change in the tangential components of the magnetization.

a) In the absence of an analyzer, we can record the equatorial Kerr effect representing the change in the reflected light intensity proportional to the change in the magnetization component perpendicular to the plane of incidence of light. If the electric vector of the light wave is perpendicular to the plane of incidence (S wave), the equatorial Kerr effect vanishes.

b) In the absence of an analyzer, we can determine the normal component of the magnetization from the change in the intensity of light reflected from a ferromagnet with polar magnetization.^[5] In this case, we have to set the plane of polarization of a polarizer in such a way that it differs from S and P, for example,

we can use a 45% orientation of the plane of polarization.

c) Proceeding as described above, we can record the presence of the horizontal component of the magnetization, which is parallel to the plane of incidence of light, from the change in the light intensity reflected from a meridionally magnetized ferromagnet.^[5]

d) In the presence of an analyzer, we can record the meridional Kerr effect representing the rotation of the plane of polarization of light proportional to the change in the component of the magnetization parallel to the plane of incidence. The meridional Kerr effect is non-zero for the P and S waves.

Summarizing the method as a whole, we can say that, in respect of the magnetic properties, the apparatus is a magneto-optic micromagnetometer,^[6] since it makes it possible to measure the magnetic properties of samples whose volume is of the order of 10^{-13} cm^3 (when the illuminated area is $1 \mu^2$ and the penetration depth of light is 1μ) and, in respect of the optical properties, the apparatus allows us to examine an object with a very high resolution ($\sim 0.2 \mu$) when the contrast is very low (the reflection coefficients of parts of the surface with different magnetizations differ by less than 0.1%). Moreover, since the method is dynamic, magnetic elements in motion can be distinguished clearly from optical inhomogeneities of the surface.

2. DETERMINATION OF THE STRUCTURE OF DOMAIN WALLS IN IRON SINGLE CRYSTALS

The question of the structure of domain walls emerging on the surface of a bulk ferromagnet has not yet been solved fully theoretically but most of the papers predict that the walls should become thinner on approach to the surface. A direct method for investigating the structure of a domain wall on the surface of a ferromagnet is the magneto-optic method,^[7] which makes it possible to determine the distribution of the magnetization directly in the volume occupied by the transition layer between the domains. As pointed out in the Introduction, a magneto-optic signal from an oscillating domain wall was observed some time ago.^[2] However, Efimov and Turpanov^[8] reported that no magneto-optic signal was produced by an oscillating domain wall and an attempt made by Kranz and Buchenau^[9] to photograph a domain wall was also unsuccessful. We are hoping that the experimental results reported below will shed some light on the subject of domain walls.

We investigated domain walls in bulk silicon-iron single crystals and on the (001) crystallographic plane of whiskers. These were 180° domain walls oriented along the [100] axis. The axis perpendicular to the sample's surface was denoted by z, that lying in the plane of the sample and perpendicular to the domain wall by x, and the one lying in the plane of the sample and directed along the domain wall by y. Then, the magnetization in two neighboring domains was $\pm J_s$, i.e., it was directed along the y and -y axes. All the curves discussed in the present section were the dependences on x, i.e., the measurements were carried out by moving the photomultiplier slit in the focal plane of the microscope across a domain wall, keeping the amplitude of the wall oscillations constant.

Figure 1 shows curves of this type obtained under different conditions. The curves on the left of Fig. 1

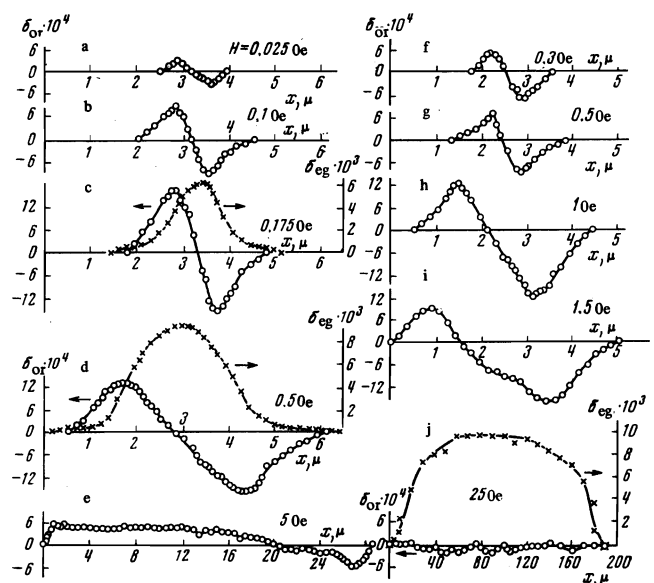


FIG. 1. Variation of the intensity of the reflected light from a region $0.35 \times 3.0 \mu$ in area on the surface of an iron whisker (a–e) and of a silicon-iron single crystal (f–j) obtained in the case of periodic oscillations of a domain wall. The curves with a reversal of the sign (open circles) represent the orientational effect δ_{Or} due to a domain wall. The equatorial Kerr effect due to domains δ_{Eq} is represented by crosses (c, d, j). The x axis lies in the plane of the sample at right-angles to the domain wall.

were obtained for whiskers and those on the right for a silicon-iron single crystal. The measurements were carried out with the photomultiplier slit adjusted to a width corresponding to the illuminated part of the sample surface ($0.35 \times 3 \mu$), which was parallel to a domain wall. The crosses in Figs. 1c, 1d, and 1j represent the "domain effect." This effect was obtained in the presence of an obliquely illuminated prism and for the perpendicular orientation of the wall relative to the plane of incidence of light (transverse orientation). In this way, we recorded the equatorial Kerr effect of a domain (case 2a in Sec. 1). The range of the nonzero equatorial effect δ_{Eq} was governed by the volume in the ferromagnet whose magnetization was reversed by the motion of the domain wall.

In this case, the effect should not have changed its sign when the slit crossed the initial position of the domain wall x_0 . Let us consider, for example, the situation when the slit was located to the right of x_0 and the effect was $\delta > 0$ when the wall moved to the right. Then, at intervals of odd half-periods, the reflected light intensity should increase by δ and at intervals of even half-periods it should remain constant. However, when the slit was located to the left of x_0 , the intensity of the reflected light should not have changed for the odd half-periods but should have changed by δ for the even half-periods. Obviously, the effects recorded in these two cases should be equal because there should be no change in the phase of the signal.

Open circles in Figs. 1a-1j represent the quadratic magneto-optic effect directly due to the oscillations of a domain wall. This domain effect could be eliminated by altering the situation described as case 1b in Sec. 1 by taking out the obliquely illuminated prism. Following the reasoning given above, we could show that the effect of a domain wall should change the sign at the point x_0 because the reflected light intensity should increase when the slit was located to the right or left of

x_0 but, in the former case, the increase should occur at odd half-periods, whereas, in the latter case, it should occur at even half-periods. Thus, the change of the sign of the effect exhibited by the dependences $\delta(x)$ provided the first proof that we were dealing with the magnetooptical signal produced by a domain wall. When the amplitude of the wall oscillations exceeded the wall thickness, the separation between the positive and negative maxima of the dependence $\delta(x)$ became equal to the oscillation amplitude. However, when this amplitude was less than the domain wall thickness, the same separation δ should have been independent of the oscillation amplitude because the positive and negative maxima of the dependence $\delta(x)$ were governed by a differential effect which appeared because of the presence of regions of maximum variation of the magnetization in the domain wall. Thus, the separation between the maxima $d = d_0$, independent of the wall oscillation magnitude, was governed by the structure of the domain wall and it was natural to regard it as the effective domain wall thickness.

Examples of such dependences $d(H)$ obtained for whiskers were given in [10]. Figure 2 shows the dependence $d(H)$ for a 180° wall in a silicon-iron single crystal (curve 2) and the dependence $d(H)$ for a domain wall in whiskers (curve 1) showing the linear dependence of the oscillation amplitude on the magnetic field in the range of stronger magnetic fields. The results obtained for different samples indicated that the thickness of a 180° domain wall in silicon-iron single crystals ranged from 0.6 to 0.8 μ .

The field dependence of the effect provided an additional support for the conclusion that the dependences $\delta(x)$ with an alternating sign were due to domain walls. For example, it is clear from Figs. 1e and 1j that a considerable reduction in the oscillation amplitude resulted, as expected, in a strong fall of the wall effect because this effect was due to a pulse signal resulting from a brief transit of a wall across the photomultiplier slit. However, the domain effect was large throughout the magnetization reversal region and reached a value δ_s corresponding to the total magnetization reversal in

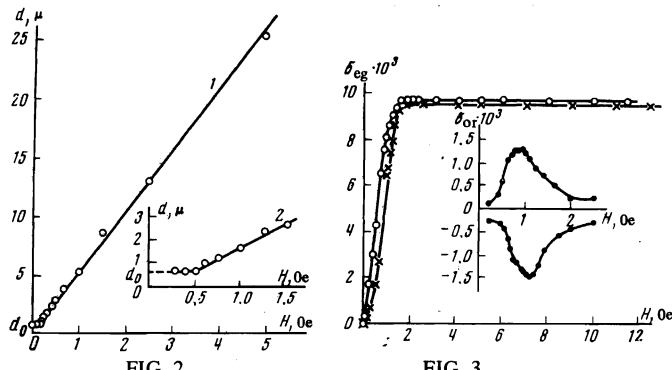


FIG. 2.

FIG. 3

FIG. 3. Field dependences of the domain and wall effects at the positive and negative maxima obtained for a silicon-iron single crystal. The open circles and crosses represent the domain effect obtained for illuminated regions of 0.35×3.0 and $1.0 \times 3.0 \mu$, whereas the black dots represent the wall effect obtained for an illuminated area of $0.7 \times 3.0 \mu$.

FIG. 4. a), b) Equatorial effect due to the transverse Néel component of a domain wall in two different regions; d), e) orientational and equatorial effects for two parts of a domain wall; c) polar Kerr effect α_K due to a domain wall; f) equatorial Kerr effect due to a domain wall and the meridional effect due to a domain in the same region.

the sample from $+J_S$ to $-J_S$. This was supported by the dependences of the domain and wall effects at the positive and negative maxima on the amplitude of the applied alternating magnetic field.

Additional information on the structure of a domain wall could be obtained by investigating other magnetooptical effects. Figures 4a and 4b show the equatorial Kerr effect of a domain wall in a whisker obtained for the parallel orientation of the wall relative to the plane of incidence of light and measured in different parts of the wall, i.e., for different values of y . The amplitudes of the positive and negative maxima were found to be governed by the transverse Néel component of the magnetization in the domain wall and the change in the sequence of the signs of the maxima of the effect shown in Fig. 4b, compared with Fig. 4a, indicated a reorientation of the wall in respect of the transverse component or, in other words, it indicated the splitting of the wall into subdomains. This was confirmed by the curves in Figs. 4d and 4e, which give the results of the simultaneous recording of the quadratic magnetooptical effect and equatorial Kerr effect in different parts of a domain wall. As expected, the sign of the quadratic effect did not change but the linear effect changed in sign between one subdomain and another.

Information on the normal component of the magnetization of a wall could be obtained by measuring the polar Kerr effect α_K (case 1a in Sec. 1). The dependence $\alpha_K(x)$ is plotted in Fig. 4c. The maximum value of α_K was approximately an order of magnitude smaller than the value α_{Ks} of iron in the visible range, [11] which indicated a strong fall of the normal (Bloch) component of J on approach to the surface. The horizontal component of J could be estimated as follows. The maximum value of the equatorial effect due to domains was 9.6×10^{-3} (Figs. 1e and 1j, and Fig. 2). The corresponding effect due to a wall should be 20% smaller because the domain effect should give rise to a nearly rectangular signal, whereas the wall effect should produce a sinusoidal signal. Next, the value obtained should be halved because of the reversal of the magnetization from $+J_S$ to $-J_S$ in the domain

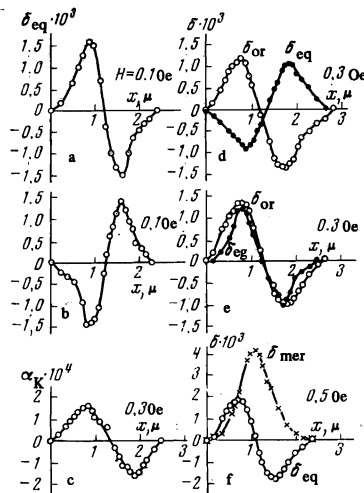


FIG. 4. a), b) Equatorial effect due to the transverse Néel component of a domain wall in two different regions; d), e) orientational and equatorial effects for two parts of a domain wall; c) polar Kerr effect α_K due to a domain wall; f) equatorial Kerr effect due to a domain wall and the meridional effect due to a domain in the same region.

effect and then it should be nearly halved again because of the continuous rotation of the magnetization vector toward a domain wall.

Thus, the maximum expected value for the transverse component of the magnetization for a pure Néel surface layer should be about 2×10^{-3} . In different cases, we obtained similar although smaller values within the range $(1.5-1.7) \times 10^{-3}$ (Fig. 4). In the case of a pure Bloch wall, the transverse component should have been completely absent and the normal component should have reached its maximum value J_S . In fact, the maximum theoretical thickness of a 180° Bloch wall should be 0.16μ . Summarizing all the results given above, we concluded that the thickness of a 180° domain wall in iron increased by a factor of 4 on approach to the surface; at the same time, the normal component of the magnetization decreased strongly and a transverse component close to J_S was observed. The surface change in the wall structure was asymmetric, i.e., the wall was bent to the right or left (which changed the polarity of different subdomains) because, in the case of a symmetric distortion of a domain wall (for example, in the case of its doubling), the average value of the transverse component, represented by the equatorial Kerr effect, should be zero. The best description of the observed results was given by a model of the change in the structure of a domain wall on the surface, put forward by Hubert^[12] for thick ferromagnetic films. According to this model, a wall should become broader on approach to the surface and not narrower—as predicted by other calculations—and although the increase in the wall thickness estimated by Hubert was only a few tens of percent, his theory predicted a further linear increase in wall thickness on the surface with increasing film thickness.

The curves in Fig. 4f represent the wall effect with an alternating sign, deduced from the equatorial Kerr effect (case 2a in Sec. 1), and the domain effect deduced from the meridional Kerr effect (case 2d in Sec. 1), in the same part of a domain wall. The transition from case 2a to the case 2d was made by introducing an analyzer.

It is worth noting the considerably asymmetry of the $\delta(x)$ curves corresponding to high oscillation amplitudes. For example, in Figs. 1e and 1i, the effect changed its sign relatively far from the middle of the interval between the positive and negative maxima. This asymmetry was systematic for large oscillation amplitudes and, therefore, it was likely to be a manifestation of a change in the structure of a moving domain wall, compared with the structure of a wall at rest. This explained the appearance of the first-harmonic signal in the vicinity of the point x_0 because a wall moving to the right differed from a wall moving to the left; it also explained the considerable asymmetry, which appeared at high oscillation amplitudes, i.e., when the velocity of a domain wall in the vicinity of x_0 became sufficiently large.

3. SUBDOMAIN MAGNETIZATION SWITCHING IN A WALL

As shown in the preceding section, a domain wall on a ferromagnet surface splits into subdomains which differ by the orientation of the transverse component of the magnetization. The splitting results from the tendency to reduce the magnetostatic energy.

We altered the subdomain structure of a wall by an external magnetic field, i.e., we studied the processes of magnetization and of switching in a domain wall. In this case, a photomultiplier slit was moved longitudinally, i.e., along the y axis. For a given value of y , we recorded the amplitude and sign of the first and second maxima of the dependence $\delta(x)$. The subdomains could then be distinguished on the basis of the sequence of positive and negative maxima. Figure 5a shows a subdomain structure obtained in this way in an arbitrarily selected part of a domain wall in some random initial state. In a $300-\mu$ long region, we observed two wide ($\sim 100 \mu$) and two narrow ($\sim 10 \mu$) subdomains. Figure 5b shows a change in the subdomain structure resulting from the application of a static magnetic field along the x axis: this field gave rise to an inequivalence of the subdomain energies because the field was directed along the transverse component J in the wall but did not cause motion of the wall as a whole since it was directed at right-angles to the domain magnetization. It should be pointed out that the effect of the field was irreversible, i.e., the subdomain size did not change when the static field was switched off. Figure 5c shows the effects of a demagnetizing alternating field with an amplitude gradually decreasing to zero. The application of this field increased the number of sub-domains and reduced their dimensions.

We also carried out experiments in which a wall was subjected to a stronger static magnetic field $H_x = +50$ and -50 Oe. In this way, it was possible to achieve a preferential magnetization of a wall in the direction of the applied field but we were unable to reach saturation magnetization in such fields.

4. DISPLACEMENTS OF DOMAIN WALLS IN ORTHOFERRITE SINGLE CRYSTALS

The domain effect described in Sec. 2 can be used to study the domain structure on the surface of bulk single crystals and the motion of domains in external magnetic fields. If the amplitude of the oscillations of a domain wall is sufficiently small, the appearance of the domain effect in the vicinity of a point x indicates that the photomultiplier slit has intersected a domain wall at this point. Examples of topographs of the domain

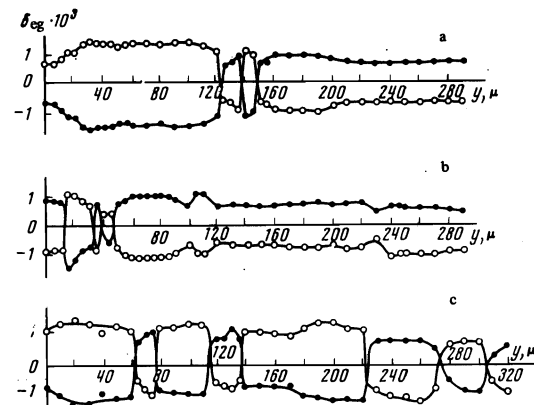


FIG. 5. Structure of subdomains in a 180° domain wall in a whisker. The open circles represent the amplitudes of the first maxima, whereas the black dots are the amplitudes of the second maxima of the dependences $\delta(x)$: a) initial state; b) after application of a static magnetic field $H = 8$ Oe along the x axis; c) after application of a demagnetizing alternating magnetic field $H = 30$ Oe.

structure on natural faces of a bulk yttrium orthoferrite single crystal are given in^[13]. In the present paper, we shall consider only the characteristic features of the magnetization processes of orthoferrite single crystals in stronger fields.

Figure 6a shows the domain effect curve obtained from the equatorial Kerr effect on the (100) face when the photomultiplier slit was moved along the [010] direction, i.e., at right-angles to the easy magnetization axis c. In this case, the slit produced a circular illuminated region of 5μ in diameter. The range where the effect differed from zero was limited to the volume of the parts of the domains in which magnetization was reversed and the simple form of the curve in Fig. 6a could be explained by the uniaxial nature of the crystal, i.e., by the fact that the domain magnetization could be directed only along the c axis ([001]). Somewhat more complex curves, obtained for a natural (101) face, are plotted in Fig. 6b. In some regions the domain effect exhibited a reversal of the sign. This could be explained by assuming that, apart from the displacement of domain walls, the magnetic field could also displace domains as a whole and this should result in the reversal of the magnetization in a certain volume in the orthoferrite, where the magnetization became opposed to the magnetic field, i.e., the reversal of the sign of the effect should be observed. One of the curves in Fig. 6b was recorded using the 45° polar Kerr effect, i.e., using the normal component of the magnetization; the other curve in Fig. 6b was obtained using the equatorial Kerr effect, i.e., using the tangential component of the magnetization. This was possible because the (101) face was inclined with respect to the c axis and, on this face, the vertical and horizontal components of the magnetization coexisted.

5. DOMAIN STRUCTURE AND SURFACE MAGNETISM OF HEMATITE

The domain structure on the surface of hematite single crystals was investigated using the method described in the preceding section. Our samples were crystals with different natural faces. Figure 7 shows the domain effect curves obtained using the equatorial Kerr effect on the (111) basal face of hematite (the

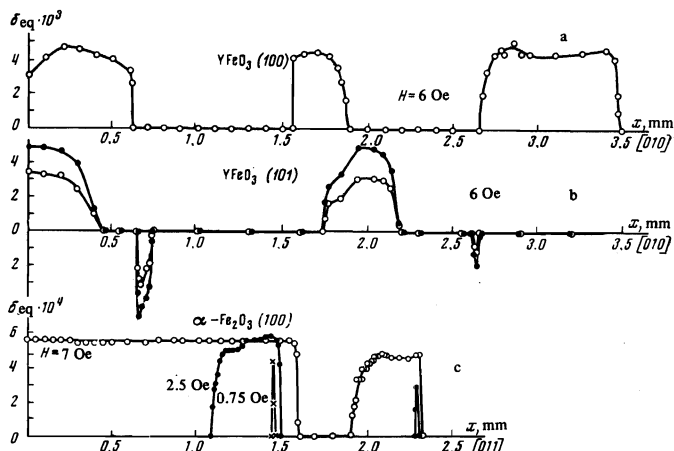


FIG. 6. Curves of the domain effect on the surface of orthoferrite (YFeO_3) and hematite single crystals: a) equatorial effect on a (100) face of YFeO_3 ; b) equatorial 45° effects on an inclined (101) face of YFeO_3 ; c) equatorial effect on a (100) face of hematite obtained for different values of the magnetic field.

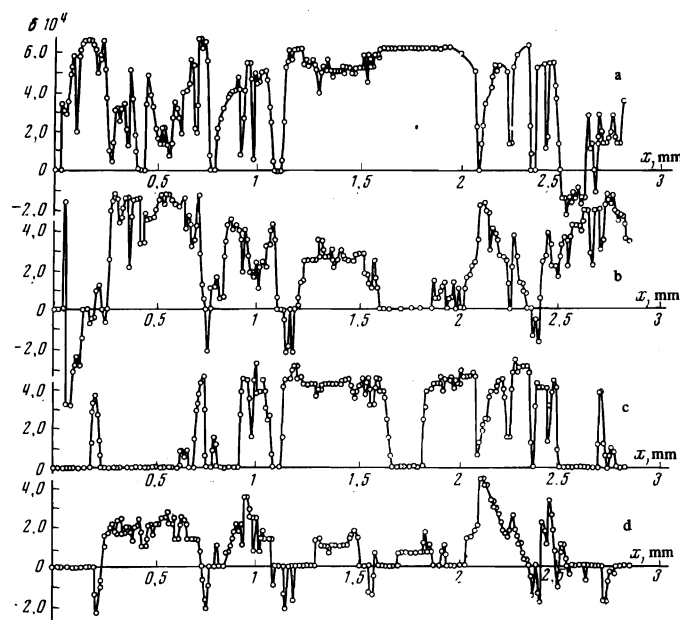


FIG. 7. Curves of the domain effect on a (111) basal face of a hematite ($\alpha\text{-Fe}_2\text{O}_3$) single crystal: a), c) magnetic field ($H = 7$ Oe) perpendicular to the plane of incidence of light; b), d) magnetic field ($H = 2$ Oe) parallel to the plane of incidence.

designation of the axes was the same as in^[14]). The curves in Figs. 7a and 7c were obtained in an external field perpendicular to the plane of incidence of light; the curves in Figs. 7b and 7d were obtained in a magnetic field parallel to the plane of incidence. The transition from a to b and from c to d was produced by rotating a sample and the magnet by 90° . All four curves were obtained by moving the photomultiplier slit along the same direction and on the same part of the surface.

Figure 7 demonstrates the complexity of the initial domain structure and of the magnetization and switching processes in hematite. The dimensions of the regions in which the magnetization switching occurred and the form of the curve $\delta(x)$ differed greatly from one region to another: the magnetization varied not only in the direction of the magnetic field but also at right-angles to this field, as indicated by the presence of a nonzero effect when the magnetic field was parallel to the plane of incidence of light (Figs. 7b and 7d); moreover, the change in sign of the domain effect in some regions indicated that the magnetization switching resulted not only from the displacement of domain walls and rotation of the magnetization vector in some domains but also from the displacement of domains as a whole. When the magnetic field was increased, the magnetization of the sample reached saturation, i.e., it reached a state in which the effect was independent of x and equal to δ_s . In the basal plane, the saturation effect was isotropic, i.e., in this case, δ_s was independent of the direction of H .

Completely different behavior was observed on a nonbasal face of hematite. Figure 6c shows curves determined for a sample with natural (100)-type faces. The results in Fig. 6c indicate that the domain structure on this nonbasal face of hematite was simple compared with the structure on the basal face and the curves in Fig. 6c were similar to those obtained for a weak ferromagnet with an easy anisotropy axis (orthoferrite), shown in Fig. 6a. However, in contrast to the

orthoferrite, the hematite sample showed no magnetization perpendicular to the surface, which was deduced from the absence of the polar Kerr effect on the (100) face. The absence of the polar Kerr effect and the characteristic anisotropy of the equatorial effect were explained in^[14] by a hypothesis of the appearance of a surface magnetism, i.e., by the appearance of a magnetic transition layer in which the magnetic state differed from that in the bulk of the sample. This transition layer had the structure of a domain wall and behaved magnetically as a weak ferromagnet with an easy anisotropy axis coinciding with the line of intersection [011] of the (111) basal plane by the (100) plane, which explained the experimental results described above.

Additional evidence of the presence of surface magnetism on the (100) face of hematite was provided by the curves shown in Fig. 8. The black dots in this curve represent the dependence of the equatorial effect on the angle of rotation of a sample, relative to the plane of incidence of light, about an axis perpendicular to the (100) plane. Zero value of the angle corresponds to the position of the sample in which the [011] direction coincided with the plane of incidence of light. In this case, the magnetic field was in the (100) plane and perpendicular to the plane of incidence of light. The dashed curve represents the projection of the magnetization vector in the bulk of the sample onto the H direction, calculated allowing for the fact that the angle between the (100) and (111) planes was $57^{\circ}35'$. This should be the dependence of the effect on the angle β if the magnetization of the sample on the surface and in the bulk were the same. This curve was normalized to the maximum of the equatorial effect. The open circles in Fig. 8 show the dependence of the equatorial effect on the rotation of the magnetic field in the (100) plane when the sample was kept fixed. Zero value of the angle corresponds to the situation in which the magnetic field was directed perpendicularly to the plane of incidence of light and parallel to the [011] axis. The direction of the magnetic field changed at $\beta = 90^{\circ}$ and the equatorial effect should have changed its sign. The corresponding calculated curve for the bulk magnetization is shown dashed. In this case, the dashed curve represents the change in the projection of the magnetization vector in the bulk onto the [011] direction.

The magnetic field used in these experiments was

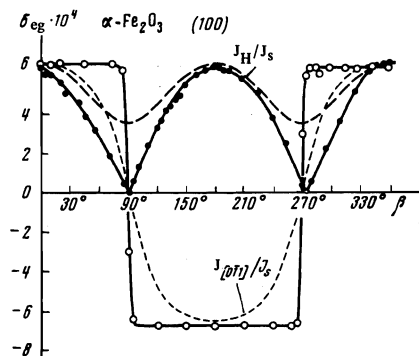


FIG. 8. Dependences of the projections of the surface magnetization onto the magnetic field direction, obtained by rotating a sample (black dots), and onto the [011] axis, obtained by rotating the magnetic field (open circles). These dependences were determined using the equatorial Kerr effect. The dashed curves are the results of calculations for the same components of the magnetization in the bulk of a sample.

50 Oe and the illuminated region was a circle of 5μ diameter. The experiments described above indicated clearly that a uniaxial weak surface ferromagnetism of the orthoferrite type appeared on the (100) face of a weak ferromagnet with an easy anisotropy plane. This was particularly clear when H was rotated and the external magnetic field passed through the direction perpendicular to the easy anisotropy axis [011] and it led to the reversal of the surface layer magnetization from $+J_S$ to $-J_S$ along the same easy axis.

It should be noted that the polar Kerr effect, i.e., the emergence of the normal component of the magnetization on the surface, was observed in very small regions (narrow strips $\sim 20 \mu$ wide) on the (100) face; these regions corresponded to the sharp peaks in Fig 6c, i.e., they were located in the region of formation of magnetization-reversal nuclei. This demonstrated a change in the nature of the surface magnetism in or its absence from these regions.

6. STRUCTURE OF DOMAIN WALLS IN HEMATITE

The method for investigating the structure of a domain wall described in Sec. 2 was applied by us to domain walls in hematite. Domain walls in weak ferromagnets with an easy-plane anisotropy should be convenient objects for investigation in view of the expected considerable wall thickness. This is due to the fact that the appearance of thick Neel walls is, in this case, unhindered by the anisotropy energy (because the magnetization vectors may be rotated from one domain to another without emerging from the easy anisotropy plane) or the magnetostatic energy (because the magnetization of a weak ferromagnet is several orders of magnitude lower than the magnetization of conventional ferromagnets and ferrimagnets and the magnetostatic energy is proportional to the square of the magnetization). On the other hand, the absence of a preferred easy anisotropy axis and the low energy of domain walls may complicate (as shown in the preceding section) the domain structure so much that it is very difficult to follow changes in one domain wall. However, after examination of several crystals with the aid of our magnetooptic apparatus, we were able to study a small (111) face on which the domain effect in weak fields appeared only in the vicinity of two lines relatively distant from another. The line located approximately in the middle of the sample behaved as a domain wall separating two domains. The size of the magnetization-reversal region increased with rising amplitude of the alternating magnetic field and the boundary moved to the right when a small static magnetic field was applied; reversal of the sign of the static field caused the boundary to move to the left. The displacement of the boundary became nonlinear in a relatively weak field and the displacements to the right and left were strongly asymmetric. The domain effect disappeared from static fields of 3–5 Oe and this was interpreted as the attainment of saturation magnetization in the positive and negative directions.

This boundary was used in the determination of the dependences $\delta(x)$ using the method described in Sec. 2. Figures 9a-9d show some of the equatorial effect curves $\delta_{eq}(x)$, obtained for different amplitudes of the wall oscillations and were analogous to the $\delta(x)$ curves obtained for iron, except that, in the present case, the domain wall thickness was approximately four times greater and equal to 2.7μ . The dependence $d(H)$ for

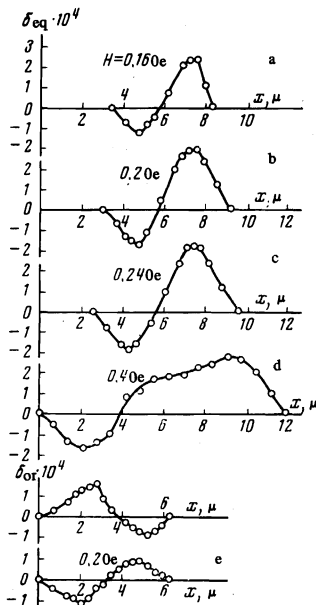


FIG. 9.

FIG. 9. a-d—Equatorial Kerr effect due to the transverse Néel component of the magnetization in a domain wall on the surface of a hematite single crystal, obtained in different magnetic fields; e—orientational effect due to a wall obtained for two mutually perpendicular orientations of the plane of polarization of light.

FIG. 10. Dependence of the separation between the positive and negative maxima of the $\delta(x)$ curves on the field causing domain oscillations (open circles) and on the width of the photomultiplier slit (black dots).

hematite is represented by open circles in Fig. 10. At high amplitudes of the wall oscillations in hematite, we also observed a strong asymmetry of the dependences $\delta_{\text{eq}}(x)$ (see, for example, Fig. 9d), discussed at the end of Sec. 2.

We were able to determine independently d_0 since the thickness of the domain wall was quite considerable. At a fixed oscillation amplitude corresponding to $H = 0.2$ Oe, we determined the dependences $\delta_{\text{eq}}(x)$ for a variable slit width l . As expected, when the slit width was equal to or less than the domain wall thickness, d ceased to depend on the slit width and became equal to d_0 (black dots in Fig. 10).

Figure 9e shows the orientational effect dependences $\delta_{\text{or}}(x)$ for a wall in hematite obtained for two mutually perpendicular orientations of the plane of polarization of linearly polarized light. Since the measured effects were comparable in these two cases, we concluded that the domain wall was of the 120° and not 180° type. A similar symmetric situation was observed for iron whiskers for 90° closure domains only. However, in the experiments on 180° walls, described in Sec. 2, the quadratic effects obtained for two mutually perpendicular polarizations of light were quite different in magnitude. For example, when a 180° domain wall was perpendicular to the plane of polarization of light (case I), the effect of the wall was large, whereas in case II, when the light-wave vector e was parallel to the domain wall, the effect was very small.

This could be explained qualitatively as follows: in the absence of an obliquely illuminated prism, the inci-

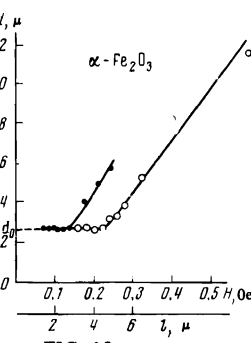


FIG. 10.

dent beam included not only rays with angles of incidence of arbitrary value and sign but also rays with arbitrarily oriented planes of incidence. Therefore, although the polarization of light was fixed (linear), the incident beam included all types of polarization of light from S to P. The cases described above differed because, in case I the plane of incidence of light for the P wave was perpendicular, whereas in case II it was parallel to the domain magnetization. The P wave dominated the quadratic orientational effect at large angles of incidence.^[15] Therefore, the results obtained for a 180° domain wall in iron could be explained qualitatively by assuming that, in case I, the transition from the bulk of the domain to its wall resulted in a greater average change in the refractive index Δn than the corresponding change in case II. An estimate of the change in the refractive index in the isotropic case $(\Delta n_{||})_{100} = (\Delta n_{||})_{111}$ and for a domain wall oriented in the (001) plane along the [100] axis confirmed this explanation qualitatively; quantitative estimates would require a knowledge of the constants $(\Delta n_{||})_{100}$ and $(\Delta n_{||})_{111}$ for iron.

¹ G. S. Krinchik, G. M. Nurmukhamedov, and V. P. Zolotarev, *Prib. Tekh. Eksp.* No. 4, 171 (1964).

² G. S. Krinchik and A. N. Verkhozin, *Zh. Eksp. Teor. Fiz.* 51, 1321 (1966) [*Sov. Phys.-JETP* 24, 890 (1967)].

³ G. S. Krinchik and V. A. Krylova, *ZhETF Pis'ma Red.* 16, 267 (1972) [*JETP Lett.* 16, 188 (1972)]. G. S. Krinchik, V. A. Krylova, E. V. Berdennikova, and R. A. Petrov, *Zh. Eksp. Teor. Fiz.* 65, 715 (1973) [*Sov. Phys.-JETP* 38, 354 (1974)]; G. S. Krinchik, Trudy mezdunarodnoi konferentsii po magnetizmu (Proc. Intern. Conf. on Magnetism), Vol. 1, Moscow, 1973.

⁴ G. S. Krinchik and V. S. Gushchin, *ZhETF Pis'ma Red.* 10, 35 (1969) [*JETP Lett.* 10, 24 (1969)]; G. S. Krinchik and E. E. Chepurova, *ZhETF Pis'ma Red.* 11, 105 (1970) [*JETP Lett.* 11, 64 (1970)].

⁵ G. S. Krinchik and E. E. Chepurova, Trudy mezdunarodnoi konferentsii po magnetizmu (Proc. Intern. Conf. on Magnetism), Vol. 1, Moscow, 1973.

⁶ G. S. Krinchik, Sb. Problemy magnetizma (Collection: Problems in Magnetism), Nauka, M., 1972, p. 133.

⁷ G. S. Krinchik, *Fiz. Metal. Metalloved.* 3, 549 (1956).

⁸ V. I. Efimov and I. A. Turpanov, *Izv. Vyssh. Uchebn. Zaved. Fiz.* No. 6, 82 (1971).

⁹ J. Kranz and U. Buchenau, *IEEE Trans. Magn. MAG-2*, 297 (1966).

¹⁰ G. S. Krinchik and O. M. Benidze, *ZhETF Pis'ma Red.* 18, 281 (1973) [*JETP Lett.* 18, 165 (1973)].

¹¹ G. S. Krinchik and V. A. Artem'ev, *Zh. Eksp. Teor. Fiz.* 53, 1901 (1967) [*Sov. Phys.-JETP* 26, 1080 (1968)].

¹² A. Hubert and Z. Angew, *Phys.* 32, 58 (1971).

¹³ O. M. Benidze and A. V. Zalesskii, *Fiz. Tverd. Tela* 15, 2207 (1973) [*Sov. Phys.-Solid State* 15, 1471 (1974)].

¹⁴ G. S. Krinchik, A. P. Khrebtov, A. A. Askochenski, and V. E. Zubov, *ZhETF Pis'ma Red.* 17, 4 (1973) [*JETP Lett.* 17, 2 (1973)].

¹⁵ G. S. Krinchik and E. A. Gan'shina, *Zh. Eksp. Teor. Fiz.* 65, 1970 (1973) [*Sov. Phys.-JETP* 38, 983 (1974)].

Translated by A. Tybulewicz

232